Charge-density-wave-phase—mode evidence in one-dimensional $K_{0.3}MoO_3$

G. Travaglini and P. Wachter
Laboratorium für Festkörperphysik, Eidgenössische Technische Hochschule Zürich—Hönggerberg, CH-8093 Zürich, Switzerland
(Received 17 February 1984)

Reflectivity measurements in the far-infrared region irrefutably show the consequence of the Peierls instability in the blue bronze $K_{0.3}MoO_3$ system. At 5 K, a very strong polarization-dependent phonon spectrum is observed: At photon energies below 8 meV, a giant, nearly undamped structure dominates the whole spectrum polarized along the b axis. The structure, reaching reflectivity values of 97%, is assigned to the oscillation of the pinned Fröhlich charge-density-wave (CDW) (A_-) mode. Optical constants are calculated by means of the Kramers-Kronig relation. The results are compared to the predictions of mean-field theory ($m^*_{\rm CDW}, \lambda, T_c^{\rm MF}$) and to the experimental results on $K_2Pt(CN)_4Br_{0.3}\cdot 3H_2O$ (KCP). No softening of the A_- mode or of the CDW energy-loss spectrum was observed. A midgap absorption can be related to the presence of solitons (dislocations in CDW lattice) and will be discussed with the latest results on the non-Ohmic conductivity.

INTRODUCTION

Peierls[1] argued that a one-dimensional (1D) metal is unstable with respect to a lattice distortion with a modulation π/k_F and that there would be a new reciprocal-lattice vector creating an energy gap at the Fermi level, transforming the high-temperature metallic to a low-temperature insulating state. Fröhlich[2] showed that the Peierls periodic lattice distortion needs a rearrangement of the electronic density of states which interacts with the lattice to balance the lattice restoring forces; this rearrangement gives rise to an electronic charge-density wave (CDW).

The most studied one-dimensional compounds in the past few years are $K_2Pt(CN)_4Br_{0.3}\cdot 3H_2O$ (KCP) and the tetracyanoquinodimethanide (TCNQ) salts,[3] which have served as model systems for study of the Peierls instability and the Fröhlich collective mode. Recently two new transition-metal trichalcogenides, $NbSe_3$ (Refs. 4 and 5) and TaS_3, have become important[6,7] in connection with the dimensionality phenomena. A transition-metal oxide, the so-called blue bronze $K_{0.3}MoO_3$, instead, is a very old material[8] (1964), but only in the last three years has it been recognized to have 1D properties because of optical measurements.[9] The term bronze has been given to a group of highly doped metal oxides which in many cases have a metallic luster.

$K_{0.3}MoO_3$ belongs to the class of ternary transition-metal oxides $M_xT_aO_b$ incorporating variable amounts x of a third element M, where M is usually an alkali or alkaline-earth metal, which donates its electron(s) to the conduction band of the host metal. It has been proposed previously that the band structure should be similar to the one of ReO_3 (Refs. 9—11); thus in the blue bronze the conduction band is made up of a combination of antibonding t_{2g} orbitals from the host metal and oxygen p_π orbitals. The blue bronze $K_{0.3}MoO_3$ is well known for its metal-semiconductor transition at $T_c = 180$ K,[12] whereas the red bronze $K_{0.33}MoO_3$ (Refs. 13 and 14) is a highly anisotropic semiconductor at all temperatures.

The blue bronze crystal structure is face-centered monoclinic with space group $C2/m$, where corner-sharing MoO_6 octahedra form infinite sheets, separated by K ions.[15] Single crystals of this material cleave parallel to the monoclinic b axis and to the [102] direction. The MoO_6 layers are built by clusters of ten distorted octahedra-sharing edges, being linked by corners in the [010] and [102] directions. These clusters ($K_3Mo_{10}O_{30}$) are arranged in columns along the b axis (metallic) and steplike along the [102] direction (semiconductorlike); the unit cell contains two clusters or 20 formula units.

Polarized optical-reflectivity measurements first revealed that $K_{0.3}MoO_3$ can be considered as a quasi 1D conductor and that the phase transition at 180 K can be understood to be of the Peierls type.[9] Optical spectroscopy is an ideal technique to investigate the macroscopic consequences of the Peierls transition, such as a CDW. Lee *et al.*[16,17] and Rice and Strässler[17] have shown that whenever the CDW is pinned to lattice points or impurity potentials, a strong peak in the ac conductivity is expected instead of the Fröhlich superconductivity for an incommensurate CDW. There are two modes $A_\pm$ which arise from linear combinations of $q_0 = \pm 2k_F$ phonons of the CDW. The A_+ mode depicts an amplitude oscillation of the CDW and the A_- mode corresponds to an oscillation of the CDW phase.

Raman scattering measurements have been found to be suitable to study the A_+ mode; the amplitude mode does not move the CDW nodes and thus does not induce a dipole moment as the CDW-phase mode A_- does. If the structure symmetry has an inversion center as is the case for the blue bronze the A_+ mode cannot be observed by means of infrared spectroscopy. First in the Krogmann salt KCP (Ref. 18) and recently in $K_{0.3}MoO_3$,[19] the CDW-amplitude mode A_+ was indeed found by means of Raman scattering. The observation of diffuse x-ray

scattering[20] at an incommensurate wave vector at 110 K and the nonlinear conductivity[21] of the blue bronze have supported the ideas of Ref. 9 and corroborate the results of Ref. 19. The very strong electron-phonon coupling results in a giant Kohn[22] anomaly of an acoustic longitudinal phonon mode which condenses at temperatures below the critical temperature T_c, giving rise to the distorted phase (crystallographic superstructure of period π/k_F).

As in KCP (Ref. 23) the Kohn anomaly has also been found in the blue bronze.[24] The purpose of this paper is the optical investigation of the CDW-phase mode A_- in the blue bronze system. A discussion within the mean-field-theory predictions[16,17] and a comparison with KCP (Refs. 25–27) results are made.

REFLECTIVITY MEASUREMENTS

The optical reflectivity of a large single crystal of $K_{0.3}MoO_3$ has been measured in an extended photon-energy range from 12 eV down to 1 meV using linearly polarized light, in a temperature region between 5 and 300 K. In the far-infrared (FIR) part of the spectrum we have used a Bruker Fourier spectrophotometer with triglicyne sulfate detectors down to 25 cm^{-1} and with a liquid-helium-cooled germanium bolometer from 100 to 8 cm^{-1}. As in Ref. 9 the incident light was polarized parallel to the metallic b axis and perpendicular to the [102] direction.

The whole spectrum is shown in Fig. 1; one notes that for $\vec{p}||b$ the room-temperature spectrum is metal-like with a plasma edge at about 1.3 eV and a reflection shoulder at 0.2 eV. For temperatures below $T_c = 180$ K the metal-like reflectivity turns into a semiconductorlike spectrum shown for $T = 5$ K in the same figure; the shoulder at 0.2 eV has become a broad reflection maximum and typical phonon lines appear for photon energies below 0.12 eV. In the inset of Fig. 1 the low-temperature FIR reflectivity is presented in an expanded energy scale to give clear evidence of the phonon spectrum.

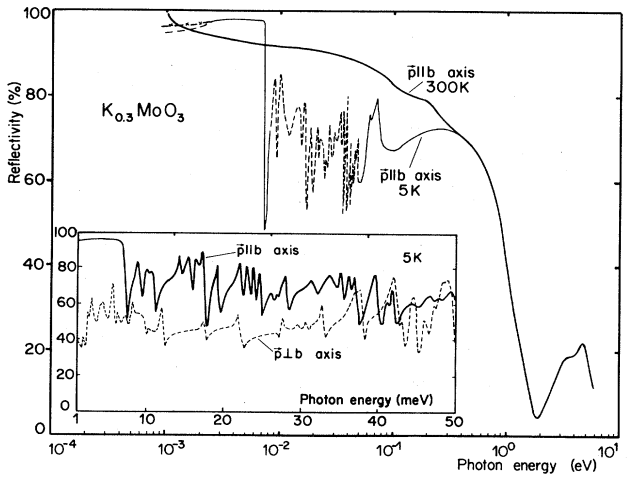

FIG. 1. Polarized reflectivity of $K_{0.3}MoO_3$ at 5 and 300 K; note the very strong structure in the FIR and the two possible $\omega \to 0$ extrapolations.

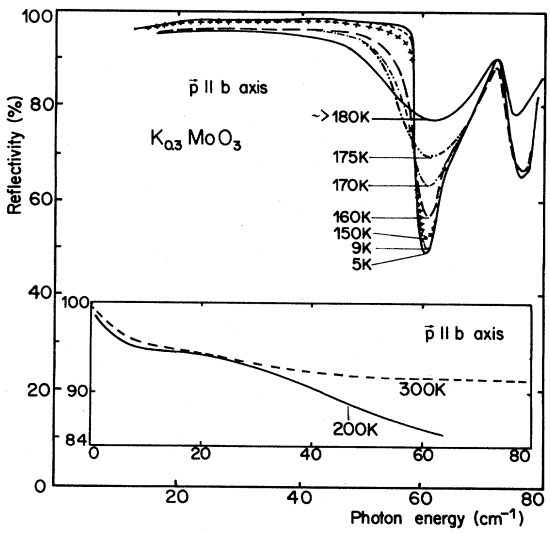

FIG. 2. Temperature dependence of the reflectivity observed in the FIR for light polarized parallel to the conducting axis; the structure is assigned to the pinned Fröhlich mode.

Since the consequences of the higher-energy reflectivity spectrum have been discussed before,[9] we now concentrate only on the FIR region of the spectrum and mainly on photon energies below 8 meV and for $T < T_c$. In this region a very high reflectivity peak which reaches a value of 97% stands out from the other maxima (the dashed part of the 5-K curve is the $\omega \to 0$ extrapolation). The purpose of this paper is to study the correlation of this giant peak and the 1D properties of the blue bronze, particularly the pinned Fröhlich mode (CDW-phase mode).

The temperature dependence of this unusual maximum is shown in Fig. 2. A very weak change (4%) occurs between 5 and 180 K in the plateau region corresponding to the transverse frequency region (ω_{TO}) of the A_- mode. In contrast, the region of the reflectivity dip, corresponding to the longitudinal region (ω_{LO}) of the A_- mode shows a very drastic temperature dependence (30%). The damping of this longitudinal oscillation increases dramatically as the temperature reaches the critical temperature T_c of 180 K.

The reflectivity behavior above T_c is presented in a more expanded reflectivity scale in the inset of Fig. 2. Some samples also show a weak maximum at 200 K in the same energy region which disappears at room temperature. With the help of the dc conductivity[28] of the material below T_c we can, according to the Hagens-Rubens relation, extrapolate the reflectivity to 100% as $\omega \to 0$.

KRAMERS-KRONIG TRANSFORMATION

The spectra have been analyzed by means of the Kramers-Kronig relation with suitable standard extrapolations for $\omega \to \infty$,[29] and will be discussed in terms of the dielectric functions. In Figs. 3 and 4 the real part ϵ_1 and the imaginary part ϵ_2 of the dielectric function ϵ is shown as determined from the analysis of the 5-K reflectivity

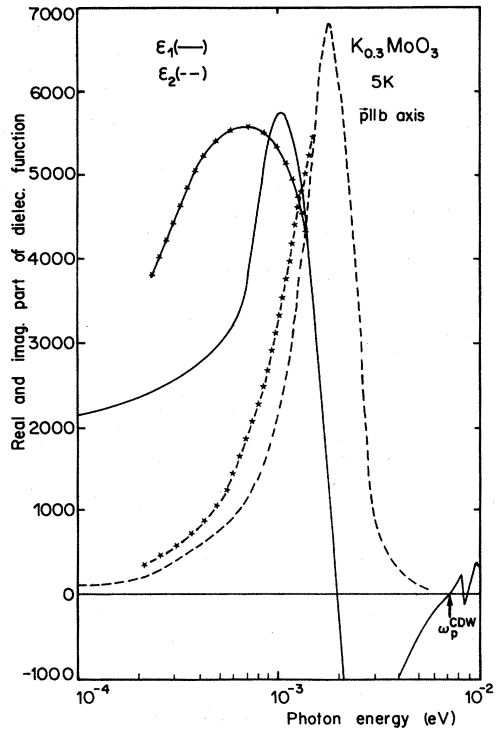

FIG. 3. Real (ϵ_1) and imaginary (ϵ_2) parts of the dielectric function of $K_{0.3}MoO_3$ in the CDW-phase—mode resonance region at 5 K. The two curves correspond to two possible extrapolations of the reflectivity for $\omega \to 0$.

spectrum for $\vec{p}||b$. The strong structure present in the dielectric functions for energies below 8 meV (Fig. 3) is due to the giant reflectivity peak in the FIR: ϵ_2 shows a strong peak at 1.8 meV (ω_{TO}) which reaches values of about 7000. Consequently ϵ_1 has a very large dispersion in the same region. It intersects the abscissa with $d\epsilon_1/d\omega > 0$, yielding ω_{LO} at 7.4 meV.

The dc values of ϵ_1 are very sensitive to the $\omega \to 0$ extrapolation of the reflectivity. The static ϵ_1 values lie between 2000 and 3000 (Fig. 3). The two sets of curves bracket the possible range of extrapolations (cf. Fig. 1). The derivation of the transversal frequency ω_{TO} of this giant structure depends somewhat on the extrapolation of $\omega \to 0$. Our measurements show for all samples that $dR/d\omega$ is positive at 5 K in the energy region between 10 and 15 cm^{-1}, and extrapolations for $\omega \to 0$ have been made as shown in Fig. 1. The resulting energy $\hbar\omega_{TO}$ is then 1.8 meV. If we extrapolate the reflectivity curve for $\hbar\omega < 15$ cm^{-1} with a zero slope ($dR/d\omega = 0$) towards $\omega = 0$, we can reduce the transversal frequency at most by a factor of 6 ($\hbar\omega_{TO} \approx 0.3$ meV), and, consequently, since ω_{LO} is independent from the extrapolation, the oscillator strength will be enhanced. An extrapolation for $\hbar\omega < 15$ cm^{-1} with $dR/d\omega < 0$ and $R = 100\%$ at $\omega = 0$ produces two structures: the first with $\hbar\omega_{TO} = 0$ meV and $\epsilon_2 \to \infty$ (Drude behavior), and the second at $\hbar\omega_{TO} = 1.2$ meV. Such an extrapolation is, however, incompatible with the semiconducting character of the blue bronze at very low temperatures. It is also possible that other structures in the reflectivity are present for $\hbar\omega$ between 0 and 1 meV in the megahertz or gigahertz region. Such structures will not influence the results in the FIR region at all: In fact in the optical-conductivity spectrum such structures will appear as small lines with zero width compared with the optical conductivity coming from the giant structure in the FIR. However, this possible absorption in the megahertz or gigahertz region would enhance the static dielectric constant by several orders of magnitude. In Fig. 4 the dielectric constants are depicted for higher energies in an expanded scale (for clarity ϵ_2 is not represented in the phonon region). In this figure we clearly recognize the abscissa intersections of ϵ_1; the first intersection at 7.4 meV as well as the last one at 1.35 eV, both with $d\epsilon_1/(d\omega) > 0$, are important for our discussion.

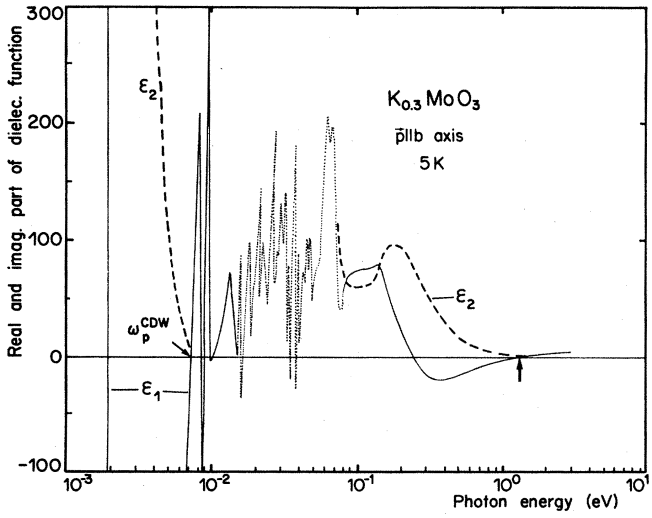

FIG. 4. Dielectric functions in the phonon region. The CDW plasma-frequency abscissa intersection is shown; the structure at about 0.2 eV is due to transitions across the Peierls gap. For clarity, in the phonon region only the more important features of ϵ_1 are reported (the structure at 0.07 eV is to be noted).

In Fig. 2 we have seen that the giant reflectivity peak for $T < T_c$ is, for some samples, still present in a reduced form at 200 K. The dispersion of such a maximum is shown in Fig. 5. ϵ_1 in the resonance region is very strongly reduced compared to the 5-K curve (from 5500 at 5 K down to 250 at 200 K) while ϵ_2 diverges as $\omega \to 0$. Even though 200 K is above the critical temperature T_c we recognize in the ϵ_1 curve strong deviations from ideal metallic properties. At 300 K the pronounced ϵ_1 structure disappears and ϵ_1 acquires very large negative values following the Drude theory for free electrons.

The complicated structures of the dielectric functions are more simplified in terms of the real part σ_1 of the optical conductivity as shown in Fig. 6. There are three strong peaks in the σ_1 spectrum at 5 K; one located at about 1.8 meV, the second centered at 0.07 eV, and the third at 0.2 eV. We assign the structure with a very high oscillator strength in the FIR region to a pinned Fröhlich $2k_F$ phase mode A_-; the structure at 0.2 eV is assigned to electronic transitions across the Peierls gap 2Δ (the struc-

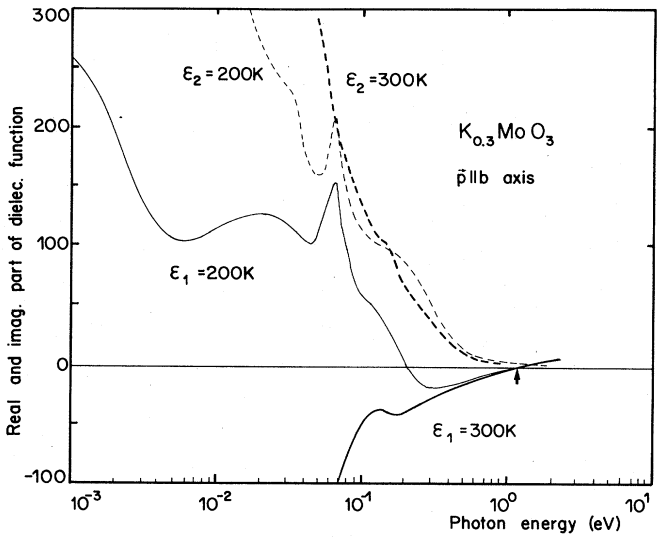

FIG. 5. Dielectric functions of $K_{0.3}MoO_3$ at 200 and 300 K. One recognizes strong deviations from free-electron behavior in the ϵ_1 structure at 200 K due to the still-present CDW mode.

ture at 0.07 eV is treated below in the discussion). The many sharp lines between these two boundary structures are due to phonon absorption. A realistic phonon analysis for $K_{0.3}MoO_3$ is very difficult, because of the large number of atoms ($K_6Mo_{20}O_{60}$) in the primitive cell.

The very low symmetry of the blue bronze structure ($C2/m$) permits at the Γ point roughly 60 infrared-active modes each of A_u and B_u types. In the distorted lattice, many new optical phonons are created by Brillouin-zone folding. The experimental value of $2k_F$ approaches the commensurate value $\frac{3}{4}b^*$ or $\frac{5}{4}b^*$ ($b^*=2\pi/b$) in the $K_{0.3}MoO_3$ system,[20] which implies a fourfold folding of the Brillouin zone. Some phonon lines indeed show a fourfold splitting (Fig. 1) which could effectively be related to this zone folding. The phonon spectrum polarized along the b axis has a stronger intensity than in the [102] direction.

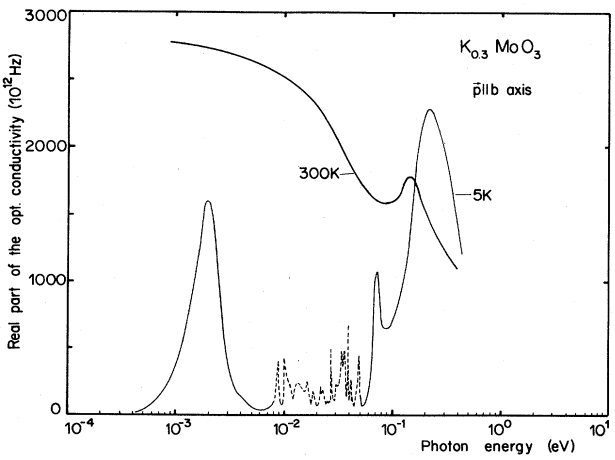

FIG. 6. Optical conductivity of the blue bronze at 5 and 300 K. The FIR structure is the resonance of the oscillating CDW.

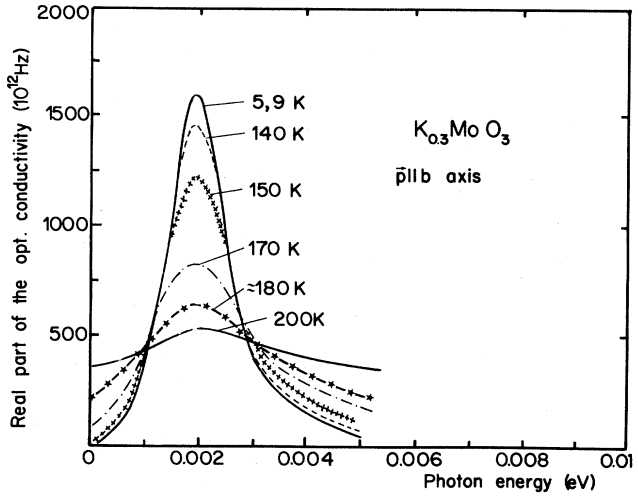

FIG. 7. Temperature dependence of the CDW optical conductivity in the FIR region.

It is possible that also present in this spectrum are phonons which have the correct symmetry for first-order coupling to the condensed carriers to generate the so-called phase phonons.[30,31] In any case the strong structure in the FIR has a weight about 10 to 20 times larger than the other phonon lines and therefore we will discuss the problem only in terms of one CDW component neglecting the small contributions of other possible components of higher order.

At 300 K the FIR CDW peak disappears and σ_1 merges into the Drude regime with a dc value of about 3000 $(\Omega\,\mathrm{cm})^{-1}$. A Peierls precursor is still present at room temperature. The high-temperature phase ($\langle\Delta\rangle=0$) consists of domains which anticipate the low-temperature ordered structure. The resonance of a pseudogap at $T>T_c$ is associated with one-dimensional fluctuations. The temperature dependence of the strong σ_1 structure in the FIR is plotted in Fig. 7. The line intensity is only weakly temperature dependent between 5 and 140 K, then the peak decreases quickly in intensity as the temperature reaches the critical value 180 K and it becomes increasingly broader to achieve an overdamped structure around 200 K.

DISCUSSION

Mean-field theory predicts a frequency softening of the CDW-amplitude A_+ mode. In $K_{0.3}MoO_3$ no softening was observed for the A_- mode and only a small frequency shift of 7 cm^{-1} was observed for the amplitude mode A_+.[19] The same conditions have also been observed in KCP.[25–27]

To analyze the low-temperature response of the pinned CDW we have used a standard oscillator model to fit the real part of the optical conductivity assuming

$$\sigma_1=\frac{1}{4\pi}\frac{\omega_p^{2\,\mathrm{CDW}}\omega^2\Gamma}{(\omega_{\mathrm{TO}}^2-\omega^2)^2+\omega^2\Gamma^2}\,,\quad \omega_p^{\mathrm{CDW}}\equiv\omega_{\mathrm{LO}}\,. \tag{1}$$

Generally the plasma frequency is defined as

$\omega_p^2 = 4\pi e^2 N/(m^* \epsilon_{opt})$, where N is the electron concentration with effective masses m^* which participate in the collective longitudinal oscillation. ω_{TO}^2 in formula (1) is proportional to the restoring force of the CDW due to the pinning potential.

The CDW plasma frequency is visualized in Fig. 4 and accentuated in Fig. 8 where the energy-loss spectrum [$\mathrm{Im}(1/\epsilon)$] of the blue bronze is reported. We recognize in Fig. 8 two principal structures: the first at 7.4 meV corresponding to the CDW longitudinal-optical frequency, and the second, a very large structure coming from the Drude part of the electronic transition across the Peierls gap. The noise structure between the two peaks is due to longitudinal-phonon frequencies.

At room temperature the coupled plasma frequency ω_p^* was found at 1.35 eV. To calculate the uncoupled plasma frequency $\omega_p = \omega_p^* (\epsilon_{opt})^{1/2}$ we have applied a Drude fit to the room-temperature ϵ_2 curve, obtaining $\omega_p = 2.7$ eV. From this one obtains the effective carrier concentration $N^* = N m_e/m^* = 5.4 \times 10^{21}$ cm^{-3}, which yields (1)m_e/m^* charges per K ion and therefore $m^* \approx m_e$.[9]

In Fig. 9 is given the number of electrons N_{eff} per unit cell connected with the electronic absorption. The curve exhibits an initial saturation plateau at about 1.3 eV. The line is obtained by decoupling the reflectivity curve from the transitions at 3.7 eV between the π, p_π valence band to empty π^* and σ^* bands (cf. Ref. 9). The saturation value for N_{eff} is about 6 electrons per unit cell. Above we have seen that a unit cell contains 20 formula units ($K_6Mo_{20}O_{60}$) and that the K ions donate all their electrons to the conduction band of the host metal. This result means that the conduction band in $K_{0.3}MoO_3$ is a nearly-free-electron band disturbed at the Fermi energy by the Peierls instability. This feature has also been found in KCP; Zeller and Bruesch[32] argued that "free electrons" are equal to "constant electron density." A nearly-constant electron density in one dimension in the KCP system is easy to achieve by a hybridization of the Pt d_z^2 orbitals with an s orbital overlapping the neighboring Pt hybridized orbitals in a σ bond. This result will therefore be a consequence of the one dimensionality of the system.

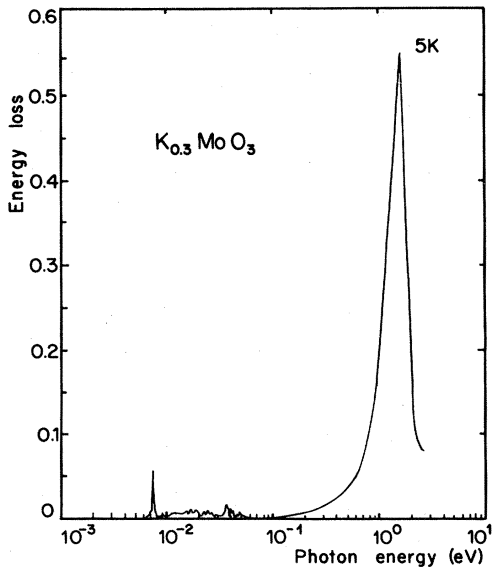

FIG. 8. Energy-loss spectrum of $K_{0.3}MoO_3$ at 5 K. The first structure is due to the CDW plasma frequency and the last to transitions across the Peierls gap.

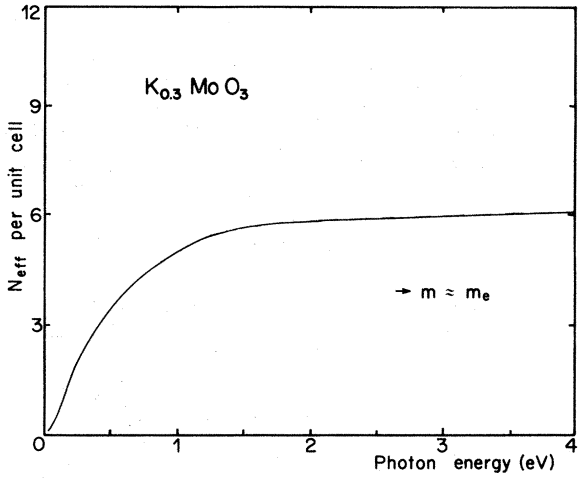

FIG. 9. Effective number of electrons per unit cell connected with the electron absorption at 300 K.

This kind of argumentation is not so evident for the blue bronze. First of all, in $K_{0.3}MoO_3$ the conduction band is built up by Mo d_{xy} orbitals overlapping the O p_π orbitals in a π^* bond (antibonding), and second, in the [102] direction inside of a cluster the kind of overlapping and bond is exactly the same as in the metallic direction.[33] A more fundamental argument is to consider the features of a 1D material. A 1D electron band has an "infinite" density of states at the band boundaries. The effective mass at the zone center is normally equal to or less than the free-electron mass. Because of the giant density of states most of the conduction electrons are located at the bottom of the band and consequently they will have a small effective mass. The integrated mass from $k = 0$ to $k = k_F$ will be around $1 m_e$ because of the high electron population at the zone center.

Turning back to the CDW plasma frequency and assuming that at 5 K all conduction electrons are condensed in the CDW, it turns out that $m_{CDW}^* = 910 m_e$, taking 6 electrons per unit cell and an estimated ϵ_{opt} of about 150 in the plasma-frequency formula. It is very hard to decouple some excitations in the FIR region because of the small energy range at disposition for any fit. ϵ_{opt} was obtained using the Lyddane-Sachs-Teller relationship:

$$\frac{\epsilon_{stat}}{\epsilon_{opt}} = \left[\frac{\omega_p^{CDW}}{\omega_{TO}} \right]^2 ,$$

where from Fig. 3, $2000 < \epsilon_{stat} < 3000$. The temperature effect on this longitudinal mode is illustrated in an energy-loss plot. Figure 10 shows a highly damped structure which becomes nearly overdamped in the neighborhood of the critical temperature (the second peak is due to a longitudinal oscillation of a normal phonon and is shown here for comparison). A similar behavior was also

observed on the Raman active A_+ mode where the damping parameter nearly diverges at $T_c = 180$ K.

The peak in Fig. 10 practically does not soften; the frequency shift is less than 4% in a temperature region between 5 and 180 K. Assuming a weak temperature dependence of ϵ_{opt} and m^* we can roughly estimate a decrease of the CDW condensed electrons of about 10% in this temperature region; this change is very weak in comparison with the expectations of a BCS theory. The anomalous damping effect of Fig. 10 is then mostly attributed to a change in the average pinning potential due to 1D fluctuations which reduce the CDW coherence length as the temperature increases or to nonlinear couplings between phase (Φ) and amplitude (α) modes[34] (for example, such a phason decay $\Phi \rightarrow \alpha + \Phi'$), rather than to CDW scattering on not-condensed electrons.

To fit the CDW response in the critical-temperature region we must take into account fluctuations since they are just as important below T_c as they are above T_c. In the fluctuation regime a particle or quasiparticle can perform an oscillation as well as a diffuse motion, and a generalization of Eq. (1) is needed.

The problem is to solve a generalized harmonic oscillator equation between two limits: At first only oscillations around the pinned state are of importance (true harmonic oscillator differential equation), and second, only diffusive motions of the CDW are of importance (diffusion differential equations). A memory function $M(t)$ ansatz which interpolates in the harmonic generalized equation between the two limits is a possible procedure to follow.[35,36]

A frequency-dependent damping Γ which leads automatically to a frequency-dependent restoring force ($\sim\omega_{TO}^2$) (causality condition), results from this procedure and Eq. (1), using the simplest asymptotic form for $M(t)=e^{-\gamma t}$, becomes

$$\sigma_1 = \frac{1}{4\pi} \frac{\omega_p^{2\,\mathrm{CDW}} \omega^2 \left[\Gamma_0 + \dfrac{\omega_0^2 \gamma}{\omega^2+\gamma^2}\right]}{\left[\left[\dfrac{\omega^2}{\omega^2+\gamma^2}\right]\omega_0^2 - \omega^2\right]^2 + \omega^2 \left[\Gamma_0 + \dfrac{\omega_0^2\gamma}{\omega^2+\gamma^2}\right]^2} \tag{2}$$

Comparison with Eq. (1) shows

$$\omega_{TO}^2 = [\omega^2/(\omega^2+\gamma^2)]\omega_0^2 , \tag{3}$$

$$\Gamma = \Gamma_0 + \frac{\omega_0^2 \gamma}{\omega^2+\gamma^2} . \tag{4}$$

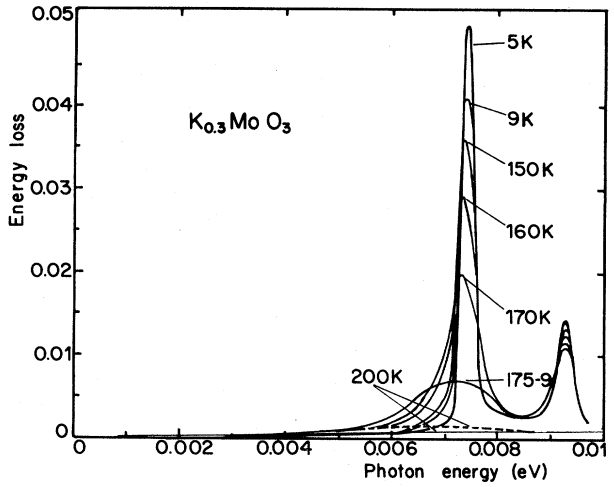

FIG. 10. Temperature dependence of the CDW energy-loss spectrum. A small softening of 4% and a very strong damping are observed from 5 up to 180 K. For 200 K two different energy-loss spectra are represented coming from two possible reflectivity extrapolations for $\omega \rightarrow 0$.

Equation (2) reduces to an oscillator equation for $\gamma = 0$ and to the standard Drude formula for $\omega_0 = 0$: $\gamma^{-1} = \Gamma - \Gamma_0/\omega_0^2$ is formally the transition time from oscillation controlled to diffusion controlled behavior. For $\omega \ll \gamma, \omega_{TO} \approx 0$, and from Eq. (2) one achieves a finite dc value,

$$(\sigma_1)_{dc}^{\mathrm{CDW}} = \frac{1}{4\pi} \frac{\omega_p^{2\,\mathrm{CDW}}}{\Gamma_0 + \omega_0^2/\gamma} . \tag{5}$$

The CDW can propagate; its motion is, however, highly damped because of fluctuations into the pinned state. At $\omega \gg \gamma, \omega_{TO} \approx \omega_0$ the CDW oscillates around its pinned position (cf. Fig. 7). The dc values obtained experimentally do not coincide with the fit values especially in the neighborhood of the critical temperature; the difference is mainly due to a single-particle conductivity which is about 70% or more of σ_{1dc}^{obs} (see Table I).

If the Fermi energy E_F is known, mean-field theory allows one to determine the dimensionless electron-phonon coupling constant λ by means of the formula

$$\Delta(0) = 4E_F e^{-1/\lambda} , \tag{6}$$

where 2Δ correspond to the Peierls energy gap at the Fermi energy E_F. There exists an augmented-plane-wave calculation of Mattheiss[37] for a hypothetical potassium molybdenum bronze K_1MoO_3 with perovskite structure

TABLE I. Comparison of the experimental values of the real part of the optical conductivity with the fit.

T (K)	ω_p^{CDW} (meV)	Γ_0 (meV)	γ (meV)	ω_0 (meV)	$(\sigma_1)_{dc}^{fit}$ (10^{12} Hz)	$(\sigma_1)_{dc}^{obs}$ (10^{12} Hz)
5	7.4	1.2	0	1.8	0	0
180	7.2	2.3	0.1	1.8	25	250
200	7.1	3.5	0.5	1.7	85	370

and lattice parameter $d=b/2$. We have calculated[38] the dispersion relation $E(\vec{k})$ (Γ—X) for one chain of $K_{0.3}MoO_3$, using an LCAO method and starting from the Mattheiss parameters for the d,p energies ϵ_d,ϵ_p and interatomic matrix elements $V_{pd\pi},V_{pd\sigma}$.

We anticipate here some results; the calculated band structure reproduces within an error of 0.1 eV the interband transitions energies described in Ref. 9. The calculation yields a conduction bandwidth of 1 eV, a Fermi energy of 0.7 eV (using the chemical electron concentration of 0.3 electrons per Mo atom), a three-quarters-filled band, $K_F=\frac{3}{4}$ $(b^*/2)$ as observed in Ref. 20, and a density of states at the Fermi level $D(E_F)$ of 2 states per eV per spin for a double-degenerate t_{2g}-p_π band (Mo d_{xz},d_{yz} orbitals). Equation (6) then yields a λ value of about 0.3 and a mean-field temperature $T_c^{\rm MF}=2.28E_Fk_B^{-1}e^{-1/\lambda}$ lying between 600 and 700 K.

It is noted that even if the kind of orbitals and bonds of $K_{0.3}MoO_3$ are completely different as in KCP, the λ parameter and $T_c^{\rm MF}$ values are quite the same. Nevertheless a stronger three-dimensional coupling as in KCP is expected in the blue bronze system because of the Mo—O bonds inside a cluster. If we compare the low-temperature curve of the optical conductivity of $K_{0.3}MoO_3$ with that of KCP,[25] it is immediately evident that the oscillator strength for transitions across the Peierls gap is reduced in the blue bronze. This is most probably due to three-dimensional coupling which reduces the discontinuity in the density of states at the gap boundaries, thus decreasing the transition-matrix element.

The knowledge of λ permits an estimate of the unrenormalized frequency Ω_q of the LA phonon which couples to the electron density. Lee *et al.*[16] have found $\Omega_q=\lambda^{-1/2}\omega_+$, where ω_+ is the CDW-amplitude—mode frequency. Introducing the experimental value $\omega_+=57$ cm^{-1} observed by means of Raman measurements,[19] we obtain $\Omega_q=13$ meV. Mean-field theory allows one to calculate the CDW effective mass

$$m^*=m_e\left[1+\frac{4\Delta^2}{\lambda\Omega_q^2}\right]\approx 800m_e\ , \tag{7}$$

which agrees quite well with $910m_e$ resulting from the CDW plasma analysis. Another interesting aspect of the low-temperature curve of σ_1 (Fig. 6) is an absorption line with a very strong oscillator strength located at about Δ (2Δ is the Peierls gap), namely, at 0.07 eV. This line has the typical feature of an excitation from a midgap state due to a topological soliton. The soliton could be present in $K_{0.3}MoO_3$ as dislocations in the charge-density-wave lattice.[39]

The partial motion of the CDW through the motion of dislocations requires a critical field $E_c\approx 1$ eV/cm. The electrical conductivity is strongly non-Ohmic when the electric field exceeds a critical field E_c. The critical field of $K_{0.3}Mo_3$ measured by Dumas *et al.* is about 0.1 eV/cm. This would only correspond to a depinning field for an incommensurate CDW pinned to a weak impurity.[39] Fleming *et al.*[40] have found by means of neutron scattering measurements on the blue bronze that the CDW, however, becomes commensurate at $0.75b^*$ below the lock-in temperature of 110 K.

Grüner *et al.*[41] have developed a model for the depinning and dynamics of a sliding CDW. For a sinusoidal pinning potential they found

$$E_c=\frac{1}{2\pi e}\lambda^{\rm CDW}m_{\rm CDW}\omega_{\rm TO}^2\ . \tag{8}$$

Introducing $m_{\rm CDW}=900m_e$ and $\lambda^{\rm CDW}\approx 4b$ we now obtain $E_c\approx 170$ KV/cm. It is not so clear if the CDW in $K_{0.3}MoO_3$ is commensurate or not, but it may be possible that the critical field observed by Dumas *et al.*[21] is related to a motion of only a part of the CDW through the presence of dislocations (solitons) in the CDW lattice. At temperatures high in comparison with T_c, inelastic neutron scattering measurements[24] exhibit a central resonance (central peak at zero energy) and a sideband phonon (soft mode). As the transition temperature is approached, the sideband phonon softens and the central component grows, ultimately carrying all the weight of the spectral function. This central resonance can be correlated with the formation of domains[42] which are also present below T_c. Their boundaries form a kind of "kink-antikink" system which can diffuse along the chain. In this case the small electrical field E_c could be connected directly to the presence of this central neutron resonance and to the presence of the very strong midgap transition in the optical conductivity σ_1. Phase oscillation of such CDW dislocations can be active at very low frequencies ($\omega\ll$Thz). In conclusion we therefore have observed the pinned Fröhlich mode in the FIR below the critical temperature. Even if the $K_{0.3}MoO_3$ crystallographic configuration does not show a 1D structure like the one of KCP, we now can classify the blue bronze as a good simple model system connected to the Peierls instability.

ACKNOWLEDGMENTS

The authors are very grateful to Professor T. M. Rice and Dr. D. Baeriswyl for reading the manuscript and for fruitful discussions. The technical assistance of J. Müller and H. P. Staub is gratefully acknowledged.

[1]R. E. Peierls, *Quantum Theory of Solids* (Clarendon, Oxford, 1955), p. 108.
[2]H. Fröhlich, Proc. R. Soc London, Ser. A **223**, 269 (1954).
[3]H. R. Zeller, in *Solid State Physics,* edited by H. J. Queisser (Vieweg, Stuttgart, 1973), Vol. 13, p. 31.
[4]P. Monceau *et al.*, Phys. Rev. Lett. **37**, 602 (1976).
[5]N. P. Ong and P. Monceau, Phys. Rev. B **16**, 3443 (1977).
[6]A. H. Thompson, A. Zettl, and G. Grüner, Phys. Rev. Lett. **47**, 64 (1981).
[7]G. Grüner *et al.*, Phys. Rev. B **23**, 6813 (1981).
[8]A. Wold, W. Kunmann, R. J., and A. Ferretti Inorg. Chem. **3**, 545 (1964).
[9]G. Travaglini, P. Wachter, J. Marcus, and C. Schlenker, Solid State Commun. **37**, 599 (1981); in *Proceedings of the International Conference on Physics of Semiconductors, Kyoto* [J. Phys. Soc. Jpn. Suppl. A **49**, 869 (1980)].
[10]J. B. Goodenough, Czech. J. Phys. B **17**, 304 (1967).
[11]M. J. Sienko, in *Non Stoichiometric Compounds,* edited by R.

F. Gould (American Chemical Society, Washington, D.C., 1963).
[12]J. H. Perlstein, Phys. Rev. B **6**, 1942 (1972).
[13]G. H. Bouchard, Jr., J. Perlstein, and M. J. Sienko, Inorg. Chem. **6**, 1682 (1967).
[14]G. Travaglini and P. Wachter, Solid State Commun. **42**, 407 (1982).
[15]J. Graham and A. D. Wadsley, Acta Crystallogr. **20**, 93 (1966).
[16]P. A. Lee, T. M. Rice, and P. W. Anderson, Solid State Commun. **14**, 703 (1974).
[17]M. J. Rice and S. Strässler, Solid State Commun. **13**, 125 (1973).
[18]E. F. Steigmeier, R. Loudon, G. Harbeke, and H. Andersen, Solid State Commun. **17**, 1447 (1975).
[19]G. Travaglini, I. Mörke, and P. Wachter, Solid State Commun. **45**, 289 (1983).
[20]J. P. Pouget, S. Kagoshima, C. Schlenker, and J. Marcus, J. Phys. (Paris) **44**, 1 (1983).
[21]J. Dumas, C. Schlenker, J. Marcus, and R. Buder, Phys. Rev. Lett. **50**, 757 (1983).
[22]W. Kohn, Phys. Rev. Lett. **2**, 393 (1959).
[23]B. Renker, H. Rietschel, L. Pintschovius, and W. Gläser, Phys. Rev. Lett. **30**, 1144 (1973).
[24]M. Sato, H. Fujita, and S. Hoshino, Solid State Phys. **16**, L877 (1983).
[25]P. Bruesch, S. Strässler, and H. R. Zeller, Phys. Rev. B **12**, 219 (1975).
[26]P. Bruesch and F. Lehnmann, Solid State Commun. **10**, 579 (1972).
[27]J. Bernasconi, P. Bruesch, D. Kuse, and H. R. Zeller, J. Phys. Chem. Solids **35**, 145 (1973).
[28]R. Brusetti, B. K. Chakraverty, J. Devenyi, J. Dumas, J. Marcus, and C. Schlenker, in Proceedings of the Annual Conference of Condensed Matter Division of the Europhysical Society, Antwerp, 1980 (unpublished).
[29]W. Beckenbaugh, J. Evers, G. Güntherodt, E. Kaldis, and P. Wachter, J. Phys. Chem. Solids **36**, 239 (1975).
[30]M. J. Rice, Phys. Rev. Lett. **37**, 36 (1976).
[31]M. J. Rice, L. Pietronero, and P. Bruesch, Solid State Commun. **21**, 757 (1977).
[32]H. R. Zeller and P. Bruesch, Phys. Status Solidi B **65**, 537 (1974).
[33]G. Travaglini and P. Wachter, Solid State Commun. **47**, 217 (1983).
[34]S. Kurihara, J. Phys. Soc. Jpn. **48**, 1821 (1979).
[35]R. Kubo, Rep. Prog. Phys. **29**, 255 (1966).
[36]P. Bruesch, S. Strässler, and H. R. Zeller, Phys. Status Solidi A **31**, 217 (1975).
[37]L. F. Mattheiss, Phys. Rev. B **6**, 4718 (1972).
[38]G. Travaglini and P. Wachter (unpublished).
[39]P. A. Lee and T. M. Rice, Phys. Rev. B **19**, 3970 (1979).
[40]R. M. Fleming (private communication).
[41]G. Grüner, A. Zawadowski, and P. M. Chaikin, Phys. Rev. Lett. **46**, 511 (1981).
[42]T. Schneider and E. Stoll, Phys. Rev. Lett. **35**, 296 (1975).